

Postindustrial enhancement of aragonite undersaturation in the upper tropical and subtropical Atlantic Ocean: The role of fossil fuel CO₂

*Sook-Nye Chung, Geun-Ha Park, and Kitack Lee*¹

School of Environmental Science and Engineering, Pohang University of Science and Technology, Pohang, 790-784, Republic of Korea

Robert M. Key

Atmospheric and Oceanic Sciences Program, Princeton University, Princeton, New Jersey 08544

Frank J. Millero

Rosenstiel School of Marine and Atmospheric Science, University of Miami, Miami, Florida 33149

Richard A. Feely and Christopher L. Sabine

Pacific Marine Environmental Laboratory, National Oceanic and Atmospheric Administration, Seattle, Washington 98115-0070

Paul G. Falkowski

Institute of Marine and Coastal Sciences and Department of Geology, Rutgers University, New Brunswick, New Jersey 08901-8521

Abstract

The dissolution of aragonite particles in the ocean primarily depends on the degree of undersaturation of seawater with respect to that mineral. Most of the upper Atlantic Ocean, particularly north of 30°S and at depths of less than 2000 m, is supersaturated with respect to aragonite, whereas much of the deep Atlantic is undersaturated. Here we report, for the first time, shallow layers of aragonite-undersaturated water between 20°S and 15°N in the eastern tropical Atlantic. These layers are centered at 800 m and are surrounded by aragonite-supersaturated water above and below. This feature most likely results from a combination of chemical and biological processes including the uptake of anthropogenic CO₂ and the oxidation of organic matter falling from the highly productive overlying surface water. Reaction with protons resulting from these processes decreases the carbonate ion concentration and consequently the saturation state of the waters with respect to aragonite. The oceanic uptake of anthropogenic CO₂ during the industrial era has caused a significant increase in the size of the undersaturated layers. Future expansion will likely occur laterally to the west and south, where the degree of supersaturation is low compared to waters to the north. This expansion of the undersaturated layers is a prime example of how human activity during the industrial era has altered the upper ocean chemistry by injecting fossil fuel CO₂ into the ocean.

The saturation state of seawater with respect to aragonite (Ω_A) under in situ conditions of temperature, salinity, and pressure is defined as

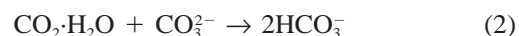
$$\Omega_A = [\text{Ca}^{2+}][\text{CO}_3^{2-}]/K_{A,SP}^* \quad (1)$$

¹ Corresponding author (ktl@postech.ac.kr).

Acknowledgments

We wish to thank Rik Wanninkhof of Atlantic Oceanographic and Meteorological Laboratory for providing us with his insight into the oceanic carbonate system. This work was supported by grant R01-2002-000-00549-0 (2003) and R11-2003-006 from the Basic Research Program of the Korea Science and Engineering Foundation (K.L.), by the Brain Korea 21 Project in 2003 (K.L.), by the U.S. National Oceanic and Atmospheric Administration Office of Oceanic and Atmospheric Research (R.A.F., F.J.M., C.L.S.), by the U.S. National Science Foundation (R.M.K., F.J.M.), and National Aeronautics and Space Administration (P.F.). This paper was assigned to contribution Number 2583 from the Pacific Marine Environmental Laboratory.

where $K_{A,SP}^*$ is the stoichiometric solubility product for aragonite. When Ω_A is greater than 1, seawater is supersaturated with respect to aragonite, and, conversely, when Ω_A is less than 1, seawater is undersaturated. The degree of saturation decreases with increasing depth in the ocean because the solubility of aragonite increases with increasing pressure (Ingle 1975). A number of factors contribute to the increase in aragonite solubility with increasing depth. First, increasing the pressure modifies the dissociation constants of carbonic and boric acids, leading to a decrease in the pH and consequently decreases in the concentration of carbonate ion $[\text{CO}_3^{2-}]$ and the Ω_A . Second, oxidation of organic matter falling from the overlying surface layer releases CO₂, which in turn decreases the pH and $[\text{CO}_3^{2-}]$ and, as a consequence, Ω_A decreases:



The organic matter effect is generally more important in shallow waters, whereas the pressure effect dominates in deep waters. Third, the solubility of aragonite increases with decreasing temperature (Mucci 1983), although this temperature effect is small compared to the other factors. The above three factors collectively cause aragonite particles to become significantly more soluble at depth.

In the upper ocean, uptake of fossil fuel CO_2 will lower $[\text{CO}_3^{2-}]$ according to the Eq. 2, which will consequently lower Ω_A . This process has been extensively discussed (Fairhall 1973; Whitfield 1975; Broecker et al. 1979; Kleypas et al. 1999; Feely et al. 2002; Sabine et al. 2002; Chung et al. 2003). Analyses of a recently compiled global carbon dataset suggest a significant upward migration (40–200 m) of the aragonite saturation horizon in the world oceans during the industrial era (Feely et al. 2002; Sabine et al. 2002; Chung et al. 2003), largely due to the uptake of fossil fuel CO_2 . This upward migration of the aragonite saturation horizon may cause CaCO_3 particles falling from the surface to be dissolved at shallower depths than in the preindustrial era, which will influence the supply of CaCO_3 to the sediments. In this paper we describe an interesting feature of aragonite undersaturation found in the tropical and subtropical Atlantic, sandwiched between supersaturated waters. We also present possible mechanisms responsible for formation of these isolated layers of undersaturated waters. The formation of this feature is a good example of how oceanic uptake of fossil fuel CO_2 can influence the oceanic CaCO_3 cycle by changing the carbonate chemistry of the upper ocean.

Data analysis and calculation method

The WOCE/JGOFS/OACES Atlantic carbon dataset—Measurements of total alkalinity ($A_T = [\text{HCO}_3^-] + 2[\text{CO}_3^{2-}] + [\text{B}(\text{OH})_4^-] + [\text{HPO}_4^{2-}] + 2[\text{PO}_4^{3-}] + [\text{SiO}(\text{OH})_3^-] + [\text{OH}^-] - [\text{H}^+]$) and total dissolved inorganic carbon ($C_T = [\text{CO}_2^*] + [\text{HCO}_3^-] + [\text{CO}_3^{2-}]$, $[\text{CO}_2^*] = \text{H}_2\text{CO}_3 + \text{CO}_2$) used to calculate in situ Ω_A were collected as part of the World Ocean Circulation Experiment (WOCE) Hydrographic Program, the International Joint Global Ocean Flux Study (JGOFS), and the Ocean–Atmosphere Carbon Exchange Study (OACES) of the National Oceanic and Atmospheric Administration (NOAA) between 1990 and 1998. The combined Atlantic dataset includes calibrated data from 23 cruises (Wanninkhof et al. 2003) and comprises 28,639 measurements of C_T and 18,771 measurements of A_T . This same dataset has been used to estimate the inventory of anthropogenic CO_2 (Lee et al. in press) and the in situ dissolution rate of CaCO_3 (Chung et al. 2003) in the Atlantic Ocean and is available at <http://cdiac.ornl.gov/oceans/datameta.html>.

Saturation state of seawater with respect to aragonite (Ω_A)—The variation of Ω_A in the ocean (see Eq. 1) is largely determined by the in situ $[\text{CO}_3^{2-}]$ and the pressure dependence of the $K_{A,SP}^*$ because the calcium ion concentration $[\text{Ca}^{2+}]$ is approximately conservative. The in situ $[\text{CO}_3^{2-}]$ was calculated from A_T and C_T using the pressure-corrected thermodynamic constants that were found to be most consistent with calibrated field measurements (Lee et al. 2000). These constants include the carbonic acid dissociation con-

Table 1. Estimated probable errors in the calculated Ω_A caused by uncertainties in thermodynamic constants and measured parameters.

Input parameters and uncertainties (reference)	Estimated error of Ω_A
$\Delta K_{A,SP}^* = \pm 0.13$ (Mucci 1983)	± 0.022
Pressure-corrected $\Delta K_{A,SP}^* = \pm 0.19$ (Ingle 1975)	± 0.023
Measured $\Delta A_T = \pm 4 \mu\text{mol kg}^{-1}$ (Millero et al. 1993)	± 0.040
Measured $\Delta C_T = \pm 2 \mu\text{mol kg}^{-1}$ (Johnson et al. 1993)	
$\Delta pK_i^* = \pm 0.004$ (Millero 1995) (<i>i</i> : carbonic and boric acids)	± 0.018
Probable error in Ω_A	± 0.054

stants of Mehrbach et al. (1973) as refitted by Dickson and Millero (1987) and other ancillary constants as recommended by Millero (1995). The pressure effect on these dissociation constants was estimated from partial molal volume and compressibility data (Millero 1995). The values of $K_{A,SP}^*$ were taken from Mucci (1983) at a given temperature and salinity at 1 atmosphere, and the effect of pressure on $K_{A,SP}^*$ was also estimated from partial molal volume and compressibility data (Millero 1995).

The probable error of the calculated Ω_A due to uncertainties in the equilibrium constants and measured values is ± 0.054 for water at 800 m based on the following uncertainties: ± 0.13 in $K_{A,SP}^*$ the solubility product of aragonite; ± 0.19 in pressure-corrected $K_{A,SP}^*$; $\pm 4 \mu\text{mol kg}^{-1}$ in measured A_T ; $\pm 2 \mu\text{mol kg}^{-1}$ in measured C_T ; and ± 0.004 in pressure-corrected pK_i^* (*i*: carbonic and boric acids) (see Table 1). The uncertainties of the measured thermodynamic constants were taken from the original works (Ingle 1975; Mucci 1983), and those of the measured parameters were from Millero et al. (1993) and Johnson et al. (1993). The probable error due to uncertainties in thermodynamic constants and measured parameters is the square root of the sum of the squared errors.

Anthropogenic CO_2 —We calculated the in situ Ω_A for the preindustrial era using measured A_T and estimates of preindustrial C_T for waters sampled during the Atlantic CO_2 survey. An important assumption in this calculation is that A_T has not changed due to oceanic uptake of anthropogenic CO_2 . The preindustrial C_T for each sample was obtained by subtracting off the anthropogenic CO_2 concentration (Lee et al. in press), which was estimated using the modified version of ΔC^* approach developed by Gruber et al. (1996). The modified method includes a more accurate determination of the net air–sea disequilibrium for a sample using an optimum multiparameter (OMP) analysis. Details of the OMP procedure for estimating mixing coefficients are given elsewhere (Lee et al. in press).

Results and discussion

Aragonite saturation in the upper tropical and subtropical Atlantic—Figure 1a,e shows the meridional distribution of

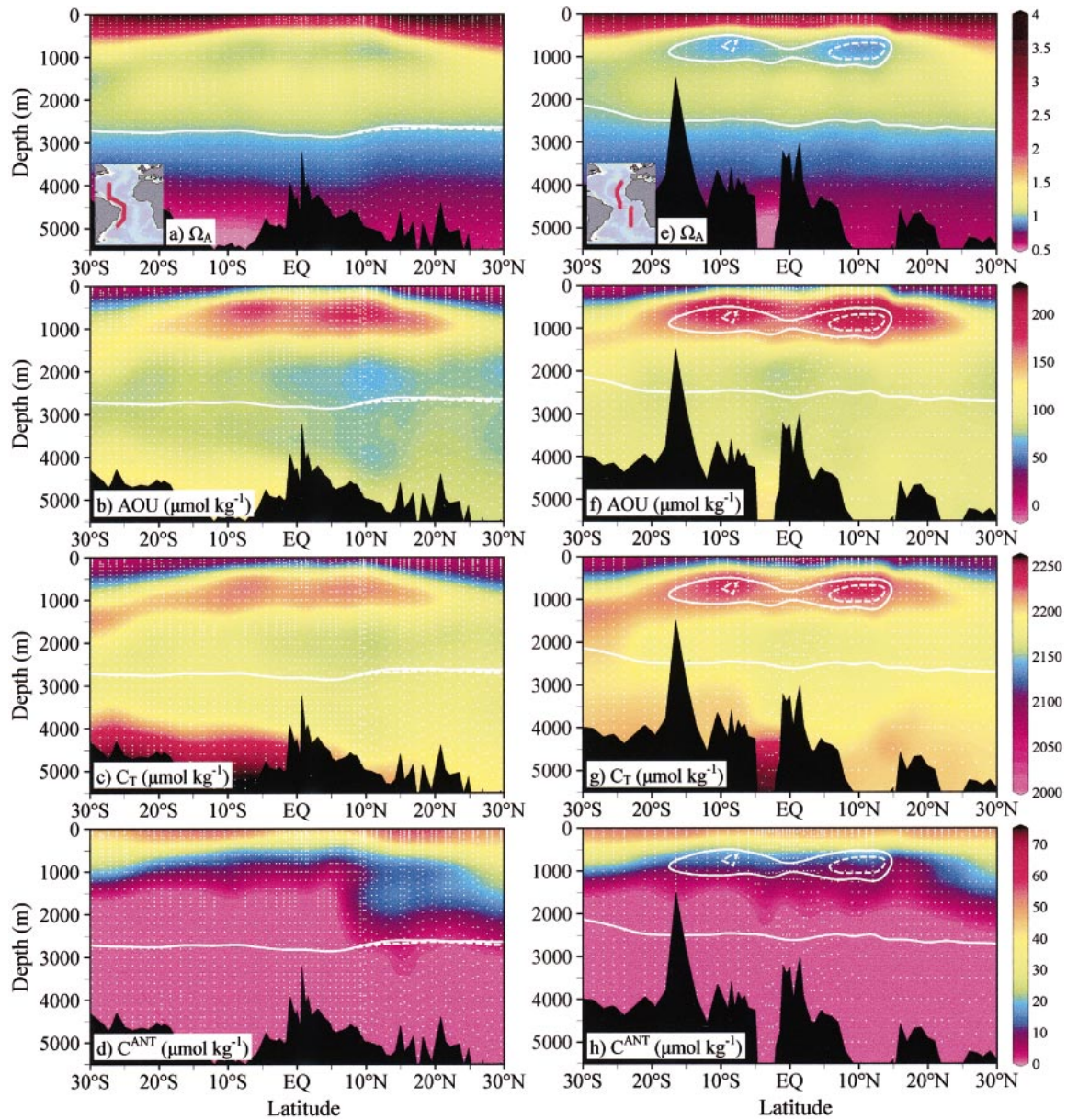


Fig. 1. The meridional distributions of (a, e) in situ aragonite saturation state (Ω_A), (b, f) apparent oxygen utilization (AOU), (c, g) total inorganic carbon (C_T), (d, h) anthropogenic CO_2 in the western (left panels) and eastern (right panels) (sub)tropical Atlantic between 30°N and 30°S . Heavy dotted and solid lines represent the aragonite saturation horizons for preindustrial era and period of measurement, respectively.

in situ Ω_A in the eastern and western (sub)tropical Atlantic between 30°N and 30°S . Water shallower than 2500 m is supersaturated by as much as 300–400% with respect to aragonite, whereas water below this depth is undersaturated. The aragonite saturation depth ($\Omega_A = 1$) is generally greater in the western than in the eastern basin because the eastern waters have accumulated more CO_2 from the oxidation of organic matter falling from the surface. The depth and areal extent of isolated layers of undersaturated water in the upper eastern tropical and subtropical Atlantic can be observed in Fig. 1e and Fig. 2c. These undersaturated layers are located at depths of 600–1100 m along 20°W from 14°N to 16°S

(hereafter called box 1) and at depths of 500–1000 m along 10°E from the equator to 20°S off the coast of Africa (hereafter called box 2). These layers are bounded above and below by supersaturated waters (Fig. 1e).

Inventories of organic matter- and fossil fuel-derived carbon in undersaturated layers—The amounts of organic matter- and fossil fuel-derived carbon that have contributed to the present state of aragonite saturation in boxes 1 and 2 were calculated separately (Table 2). The total inventory of organic matter-derived carbon (ΔC^{total}) for each latitude band of the undersaturated layer was estimated by multiply-

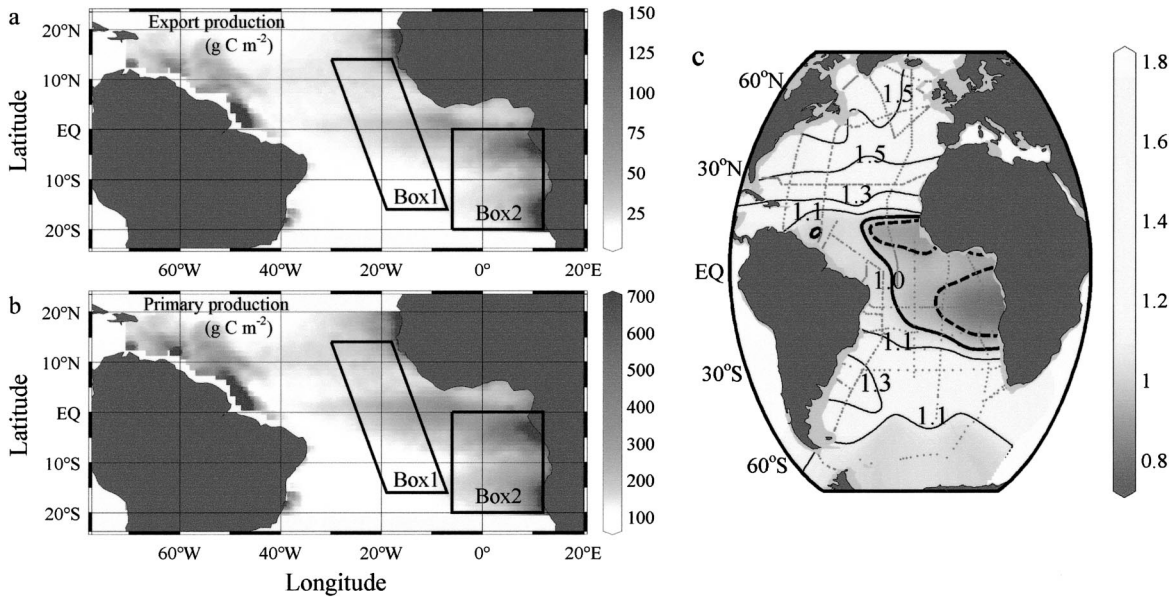


Fig. 2. (a) Export production and (b) primary production derived from data collected by the *SeaWiFS* satellite. (c) Areal extents of aragonite-undersaturated layer at 800-m depths. Black rectangles in (a) and (b) indicate the areal domains of box 1 and box 2. Laws et al.'s estimates of export production from the surface layer above box 1 and box 2 are 8.1×10^{12} mol C yr⁻¹ and 17.6×10^{12} mol C yr⁻¹, respectively. Note that Lee's estimation for the surface layer above box 1 is 7.3×10^{12} mol C yr⁻¹. The solid line in the tropics represents the areal extent of undersaturated layer for today, whereas the dotted line represents that for the preindustrial era.

ing the volume of each latitude band by differences in salinity normalized mean C_T ($\Delta NC_T^{\text{mean}}$, $NC_T = C_T \times 35/S$) or in apparent oxygen utilization (AOU = $O_2^{\text{sat}} - O_2^{\text{meas}}$, O_2^{sat} are the saturated values at the given temperature and salinity, and O_2^{meas} are the measured values) between the undersaturated water and adjacent water feeding into the undersaturated layer (Fig. 3b,c)

$$\begin{aligned} \Delta C^{\text{total}}(\text{lat. 1, lat. 2}) \\ = V(\text{lat. 1, lat. 2; long. 1, long. 2; } L, U) \times \Delta NC_T^{\text{mean}} \end{aligned} \quad (3)$$

where the mean NC_T values, NC_T^{mean} , were estimated for each

2° latitude band from the upper (U , meters in depth) to lower (L , meters in depth) boundaries of the undersaturated layer (Fig. 3b). NC_T^{mean} values for the adjacent water were predicted from fits, which are linear mixing lines between the Antarctic Intermediate Water and the North Atlantic Central Water. V is volume (km³) of water of the undersaturated layer for each latitude band (lat. 1, lat. 2; long. 1, long. 2), that is, the volume between U and L . The estimated inventories for all latitude bands were summed to produce the total organic matter-derived carbon inventory for each undersaturated layer. The $\Delta NC_T^{\text{mean}}$ -based method yields total inventories of $(15.8 \pm 4.6) \times 10^{12}$ mol C for box 1 and of $(29.6 \pm 4.4) \times 10^{12}$ mol C for box 2. In addition, the organic matter-

Table 2. Carbon budget (expressed as 10^{12} mol C) for two layers of undersaturated water with respect to aragonite in the upper tropical and subtropical Atlantic.

Parameters	Box 1	Box 2
Volume ($\times 10^6$ km ³)	2.2 (1,330 \times 3,570 \times 0.5)*	2.1 (1,920 \times 2,210 \times 0.5)*
Organic C oxidation estimated		
from NC_T	15.8 \pm 4.6†	29.6 \pm 4.4†
from AOU ($C/O_2 = 117/170$)	13.8 \pm 1.3‡	34.1 \pm 1.5‡
Anthropogenic CO ₂	26.3 \pm 4.5§	34.2 \pm 3.1§
Total C added	40.1 \pm 5.8	68.3 \pm 4.6

* Width (km) \times length (km) \times height (km).

† Error estimated using an uncertainty of ± 2 $\mu\text{mol kg}^{-1}$ in measured C_T (Johnson et al. 1993).

‡ Error estimated using an uncertainty of ± 2 $\mu\text{mol kg}^{-1}$ in measured O_2 .

§ Potential errors of anthropogenic CO₂ inventories for two boxes are estimated based on errors associated with estimating mixing coefficients from the optimum multiparameter (OMP) analysis and with defining the end member water types using the uncertainty in the calculated anthropogenic CO₂ concentration. Errors in definitions of source water types yielded an error of about 17% of the anthropogenic CO₂ inventory for each box. Detailed error analysis was described in Lee et al. (in press).

|| The total carbon added is the sum of AOU-derived carbon and anthropogenic CO₂.

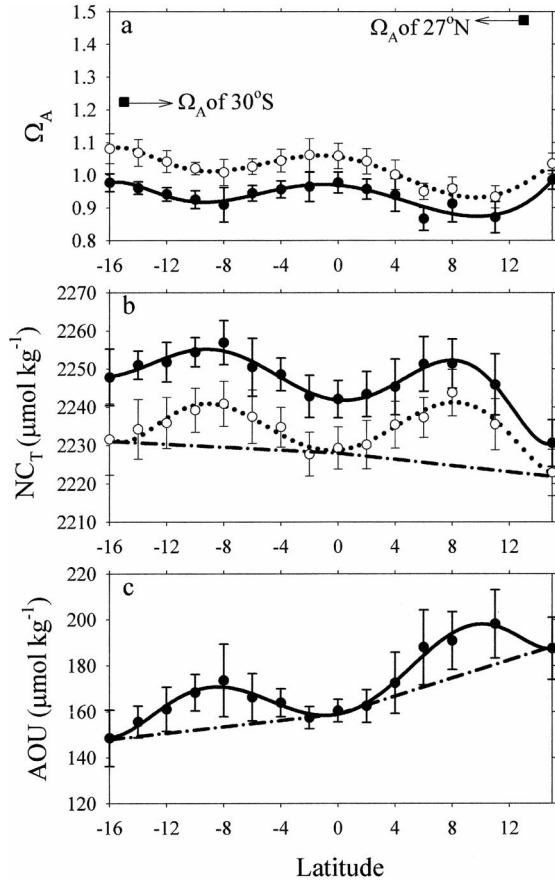


Fig. 3. Latitudinal distributions of aragonite saturation state (Ω_A), salinity ($S = 35$), normalized total inorganic carbon ($NC_T = C_T \times 35/S$), and apparent oxygen utilization (AOU) in box 1. Solid lines represent the values for today, whereas dotted lines represent those for the preindustrial era. Error bars are standard deviations from average values for each 2° latitude band. Filled squares are Ω_A values for water flowing into box 1 from the northern and southern ends. Latitudinal variations in NC_T and AOU for adjacent waters feeding into the undersaturated layer are predicted from dashed-dotted lines, which are linear mixing lines between the Antarctic intermediate water (AAIW) and the North Atlantic central water (NACW).

derived carbon inventory was separately estimated using Eq. 3 and the differences in AOU between the undersaturated water and adjacent water feeding into these layers (Fig. 3c). The AOU-based inventories of organic matter-derived carbon for boxes 1 and 2 are $(13.8 \pm 1.3) \times 10^{12}$ mol C and $(34.1 \pm 1.5) \times 10^{12}$ mol C, respectively. Thus, the independent $\Delta NC_T^{\text{mean}}$ - and AOU-based estimates are in good agreement within the uncertainties associated with each method.

The inventory of anthropogenic CO_2 (total- C^{ant}) for each 10° latitude band between lat. 1 and lat. 2 was determined by separately integrating the mean profile of anthropogenic CO_2 from U to L boundaries of the undersaturated layer:

$$\begin{aligned} \text{Total} - C^{\text{ant}}(\text{lat. 1, lat. 2}) \\ = \int_U^L A(\text{lat. 1, lat. 2; long. 1, long. 2})f - C^{\text{ant}} dz \quad (4) \end{aligned}$$

where A (lat. 1, lat. 2; long. 1, long. 2) is the area of each latitude band. The estimated inventories for all latitude bands were summed to produce the total anthropogenic CO_2 inventory for each undersaturated layer. The total amounts of anthropogenic CO_2 that have accumulated in boxes 1 and 2 are $(26.3 \pm 4.5) \times 10^{12}$ mol C and $(34.2 \pm 3.1) \times 10^{12}$ mol C, respectively, and are assumed to reflect 1994 conditions, the middle year of the Atlantic survey (Lee et al. in press). Thus, oceanic uptake of anthropogenic CO_2 and in situ oxidation of organic matter have together contributed an additional (40.1 ± 5.8) and $(68.3 \pm 4.6) \times 10^{12}$ mol C to boxes 1 and 2, respectively.

Proposed mechanisms for formation of aragonite-undersaturated layers—Comparison of the Ω_A distributions (Fig. 1a,e) with the corresponding AOU (Fig. 1b,f) and C_T distributions (Fig. 1c,g) reveals that regions of aragonite-undersaturated water coincide with regions of relatively high AOU and C_T . These correlations suggest that biological processes might, at least partially, account for the observed local reduction in the aragonite saturation state. Biological processes play a more important role in forming box 2 than box 1 (see Table 2). This is generally consistent with satellite-based estimation of higher export production from the surface layer above box 2 than box 1 (Fig. 2a) (Laws et al. 2000). A combination of higher export production from the surface layer and subsequent oxidation of organic matter results in a higher degree of undersaturation in box 2 than in box 1. The higher the export production is, the greater the amount of organic carbon available for biological oxidation will be. Export production was based on the pelagic food web model and net photosynthesis estimated from data collected by the *SeaWiFS* satellite (Fig. 2b) (Laws et al. 2000). The estimate of Laws et al. for box 1 is in reasonable agreement with that obtained by Lee (2001) for the same area by integrating the seasonal decrease in mixed layer NC_T . However, for box 2, comparison of Lee's estimate (Lee 2001) with that of Laws et al. (2000) is inappropriate, because Lee's method uses a coarse resolution (4° latitude \times 5° longitude) and misses or underestimates export production occurring near the coast of Africa. The uptake of anthropogenic CO_2 is also important in formation of undersaturated water but more or less evenly affects box 1 and box 2 (Fig. 1d,h).

The formation of isolated layers of aragonite-undersaturated water could potentially be driven by mechanisms other than increases in anthropogenic CO_2 and organic matter oxidation; however, none of the possible alternative mechanisms seems plausible. One example is mixing between different source water types flowing into this region. The southern end member is the Antarctic intermediate water (AAIW) and the northern end member is the North Atlantic central water (NACW). The AAIW appears as a low-salinity layer extending to as far as 20°N (Pickard and Emery 1982). The OMP analysis used to determine the mixing coefficients of the various source water types contributing to the waters in this region suggests that approximately 75% of the undersaturated water centered at 800-m depth in the tropical Atlantic is AAIW (Lee et al. in press). In fact, mixing between the AAIW from the south and the NACW from the north makes it impossible to produce undersaturated water

Table 3. The amount of anthropogenic CO₂ and time required to make the western tropical Atlantic and the South Atlantic undersaturated with respect to aragonite in the future.

Parameters	Western tropical Atlantic (20°N–20°S, 30°W–60°W, 500–1,100 m)	South Atlantic (20°S–40°S, 500–1,100 m)
Mean Ω_A	1.1±0.1	1.3±0.3
Mean increase* in C_T required to make each region undersaturated	11.8 $\mu\text{mol kg}^{-1}$	49.6 $\mu\text{mol kg}^{-1}$
Mean accumulation rate† of anthropogenic CO ₂	0.20±0.1 $\mu\text{mol kg}^{-1} \text{ yr}^{-1}$	0.51±0.13 $\mu\text{mol kg}^{-1} \text{ yr}^{-1}$
Mean time required to make each region undersaturated	58 yr	98 yr

* The mean increase in C_T is the difference between the present-day C_T and the future C_T that is needed to make each region undersaturated with respect to aragonite. We calculated the future C_T using the thermodynamic relationships and the assumption that the present-day A_T will not change in the future due to oceanic uptake of anthropogenic CO₂.

† The accumulation rate of anthropogenic CO₂ for each region was estimated by dividing 80% of the total anthropogenic CO₂ inventory by 45 yr; this approach assumes that 80% of the total has accumulated over the last 45 yr.

because water feeding into box 1 from the southern (AAIW) and northern (NACW) ends is actually supersaturated by approximately 120% and 147%, respectively (Fig. 3a). Similarly, mixing of the AAIW and the NACW cannot produce undersaturated water in box 2.

Geochemical consequences of lowered saturation state—The volume of the aragonite-undersaturated layer for the pre-industrial era (dotted line) (Figs. 1e and 2c) is significantly smaller than in the mid-1990s (solid line) (Figs. 1e and 2c). During the industrial era, the undersaturated layer has predominantly expanded laterally, which has led to the union of the two separate layers of undersaturated water present during the preindustrial era. Expansion of the undersaturated layer has mainly occurred in the south tropical Atlantic, largely due to considerably lower levels of oversaturation in the south compared to the north. Implicit in this conclusion is the assumption that carbon export production from highly productive overlying surface water and the amount of organic matter oxidized within this layer have not changed since the onset of the Industrial Revolution. If production has in fact increased, for example through changes in dust deposition over time, then this would contribute to the expansion of the undersaturated layer. Expansion of this undersaturated layer would likely occur laterally to the west and subsequently to the south, where the degree of supersaturation is low relative to waters to the north (Fig. 2).

We now consider the implications of the present work for the future ocean carbonate system. The mean accumulation rate of anthropogenic CO₂ in the western tropical Atlantic over the last 45 yr is 0.20 $\mu\text{mol kg}^{-1} \text{ yr}^{-1}$ (see Table 3). Assuming that anthropogenic CO₂ continues to accumulate at this rate in the future, we predict that the intermediate water (centered about 800-m depth) of the entire tropical Atlantic between 20°N and 20°S will become undersaturated with respect to aragonite by about the middle of this century (Table 3). Subsequently, undersaturation is predicted to steadily expand to the south. Similarly, the mean accumulation rate of anthropogenic CO₂ in the intermediate water of the South Atlantic is 0.51 $\mu\text{mol kg}^{-1} \text{ yr}^{-1}$, and hence this region is predicted to become undersaturated by the later part of this century (Table 3).

Continuous expansion of the undersaturated zone will increase in situ dissolution of CaCO₃ in this upper tropical and

subtropical Atlantic Ocean. This enhanced dissolution will eventually result in a greater supply of alkalinity to the surface and a smaller supply of CaCO₃ to the sediments. Enhanced shallow water dissolution of CaCO₃ is particularly important in the buffering of fossil fuel CO₂ injected into the upper ocean. Laboratory experiments (Riebesell et al. 2000) indicate that reduced supersaturation of the upper ocean slows the calcification rate of certain coccolith species. From a global perspective, a lowering of the calcification rate and an enhancement of the dissolution of CaCO₃ in the upper ocean would increase fossil fuel CO₂ storage in the upper ocean.

Analysis of inorganic carbon data compiled from the Atlantic CO₂ survey in the 1990s revealed an aragonite-undersaturation zone in the core of the Antarctic Intermediate Water that has not been noted previously and is not found in the other basins (Feely et al. 2002; Sabine et al. 2002). The aragonite-undersaturated water mass is surrounded both laterally and vertically by supersaturated waters. The accumulation of anthropogenic CO₂ and the in situ oxidation of organic matter are primarily responsible for the formation of these undersaturated layers. Future expansion of these undersaturated zones is likely to depend on the anthropogenic CO₂ accumulation rate.

References

- BROECKER, W. S., T. TAKAHASHI, H. J. SIMPSON, AND T.-H. PENG. 1979. Fate of fossil fuel carbon dioxide and the global carbon budget. *Science* **206**: 409–418.
- CHUNG, S.-N., K. LEE, R. A. FEELY, C. L. SABINE, F. J. MILLERO, R. M. KEY, J. L. BULLISTER, AND R. WANNINKHOF. 2003. Calcium carbonate budget in the Atlantic Ocean based on water-column inorganic carbon chemistry. *Glob. Biogeochem. Cycles* **17**: 1093, doi: 10.1029/2002GB002001.
- DICKSON, A. G., AND F. J. MILLERO. 1987. A comparison of the equilibrium constants for the dissociation of carbonic acid in seawater media. *Deep-Sea Res.* **34**: 1733–1743.
- FAIRHALL, A. W. 1973. Accumulation of fossil CO₂ in the atmosphere and the sea. *Nature* **245**: 20–23.
- FEELY, R. A., AND OTHERS. 2002. In situ calcium carbonate dissolution in the Pacific Ocean. *Glob. Biogeochem. Cycles* **16**: 1144, doi: 10.1029/2002GB001866.
- GRUBER, N., J. L. SARMIENTO, AND T. F. STOCKER. 1996. Anthropogenic CO₂ in the oceans. *Glob. Biogeochem. Cycles* **10**: 809–837.

- INGLE, S. E. 1975. Solubility of calcite in the ocean. *Mar. Chem.* **44**: 205–220.
- JOHNSON, K. M., K. D. WILLS, D. B. BUTLER, W. K. JOHNSON, AND C. S. WONG. 1993. Coulometric total carbon dioxide analysis for marine studies: Maximizing the performance of an automated continuous gas extraction system and coulometric detector. *Mar. Chem.* **44**: 167–187.
- KLEYPAS, J. A., R. W. BUDDEMEIER, D. ARCHER, J.-P. GATTUSO, C. LANGDON, AND B. N. OPDYKE. 1999. Geochemical consequences of increased atmospheric carbon dioxide on coral reefs. *Science* **284**: 118–120.
- LAWS, E. A., P. G. FALKOWSKI, W. O. SMITH, J. R. H. DUCKLOW, AND J. J. MCCARTHY. 2000. Temperature effects on export production in the open ocean. *Glob. Biogeochem. Cycles* **14**: 1231–1246.
- LEE, K. 2001. Global net community production estimated from the annual cycle of surface water total dissolved inorganic carbon. *Limnol. Oceanogr.* **46**: 1287–1297.
- , F. J. MILLERO, R. H. BYRNE, R. A. FEELY, AND R. H. WANNINKHOF. 2000. The recommended dissociation constants of carbonic acid for use in seawater. *Geophys. Res. Lett.* **27**: 229–232.
- , AND OTHERS. In press. An updated anthropogenic CO₂ inventory in the Atlantic Ocean. *Glob. Biogeochem. Cycles*.
- MEHRBACH, C., C. H. CULBERSON, J. E. HAWLEY, AND R. M. PYTKOWICZ. 1973. Measurement of the apparent dissociation constants of carbonic acid in seawater at atmospheric pressure. *Limnol. Oceanogr.* **18**: 897–907.
- MILLERO, F. J. 1995. Thermodynamics of the carbon dioxide system in the oceans. *Geochim. Cosmochim. Acta* **59**: 661–677.
- , J.-Z. ZHANG, K. LEE, AND D. M. CAMPBELL. 1993. Titration alkalinity of seawater. *Mar. Chem.* **44**: 153–165.
- MUCCI, A. 1983. The solubility of calcite and aragonite in seawater at various salinities, temperatures and 1 atmosphere total pressure. *Am. J. Sci.* **238**: 780–799.
- PICKARD, G. L., AND W. J. EMERY. 1982. *Descriptive physical oceanography*, 4th ed. Pergamon.
- RIEBESELL, U., I. ZONDERVAN, B. ROST, P. D. TORTELL, R. E. ZEEBE, AND F. M. M. MOREL. 2000. Reduced calcification of marine plankton in response to increased atmospheric CO₂. *Nature* **407**: 364–367.
- SABINE, C. L., R. M. KEY, R. A. FEELY, AND D. GREELEY. 2002. Inorganic carbon in the Indian Ocean: Distribution and dissolution processes. *Glob. Biogeochem. Cycles* **16**: 1067, doi: 10.1029/2002GB001869.
- WANNINKHOF, R., T.-H. PENG, B. HUSS, C. L. SABINE, AND K. LEE. 2003. Comparison of inorganic carbon system parameters measured in the Atlantic Ocean from 1990 to 1998 and recommended adjustments. ORNL/CDIAC, U.S. DOE under contract DE-AC05-00OR22725.
- WHITFIELD, M. 1975. The effect of increases in the atmospheric carbon dioxide content on the carbonate ion concentration of surface ocean water at 25°C. *Limnol. Oceanogr.* **20**: 103–108.

Received: 11 June 2003

Accepted: 9 October 2003

Amended: 3 November 2003